Bubble Point Pressures of CO2+Ethyl Palmitate by a Cubic Equation of State and the Wong-Sandler Mixing Rule

M. A. Sedghamiz, S. Raeissi

Abstract—This study presents three different approaches to estimate bubble point pressures for the binary system of CO_2 and ethyl palmitate fatty acid ethyl ester. The first method involves the Peng-Robinson (PR) Equation of State (EoS) with the conventional mixing rule of Van der Waals. The second approach involves the PR EOS together with the Wong-Sandler (WS) mixing rule, coupled with the UNIQUAC G^E model. In order to model the bubble point pressures with this approach, the volume and area parameter for ethyl palmitate were estimated by the Hansen group contribution method. The last method involved the Peng-Robinson, combined with the Wong-Sandler method, but using NRTL as the G^E model. Results using the Van der Waals mixing rule clearly indicated that this method has the largest errors among all three methods, with errors in the range of 3.96-6.22%. The PR-WS-UNIQUAC method exhibited small errors, with average absolute deviations between 0.95 to 1.97 percent. The PR-WS-NRTL method led to the least errors, where average absolute deviations ranged between 0.65-1.7%.

Keywords—Bubble pressure, Gibbs excess energy model, mixing rule, CO_2 solubility, ethyl palmitate.

I. INTRODUCTION

AS an alternative to petroleum-based diesel fuel, biodiesel has become more attractive recently because of its environmental benefits and the fact that it is made from renewable resources [1]-[4]. Analogous to conventional diesel fuel, it can be used in diesel ignition engines. The cost of biodiesel, however, is the main constraint to the commercialization of the product. Algae and used cooking oil are raw materials which can decrease the process cost, by replacing edible oils as raw material. Other factors to increase the benefits of biodiesel production are the adaption of continuous processes for transesterification and a complete separation and the recovery of valuable by-products such as glycerol [2], [5].

Biodiesel can be defined as the monoalkyl esters from long-chain fatty acids (FAE). The term biodiesel can be attributed to both long-chain fatty acid methyl esters (FAME) and ethyl esters (FAEE) [6]. Nowadays, FAME is the most commercially available biodiesel, thanks to the relatively lower price of ethanol in EU countries, whereas in countries such as Brazil and Argentina, where biodiesel ethanol (EtOH) is abundantly available with lower prices, FAEE leads the biodiesel markets [7].

There are four primary ways to make biodiesel: direct use and blending, microemulsions, thermal cracking (pyrolysis), and transesterification. The most commonly used method is the transesterification of vegetable oils and animal fats.

The transesterification reaction includes the exchange of the alkoxy group of a lipid oil or fat with an aliphatic alcohol (e.g. methanol and ethanol). This substitution will be completed in the presence of acids such as H_2SO_4 or alkalines (e.g. KOH and NaOH) as the catalyst [8]. Fig. 1 represents the biodiesel reaction scheme.
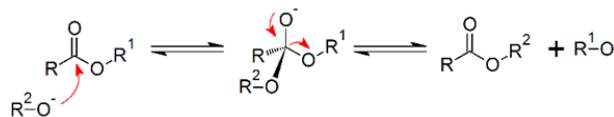

Fig. 1 Biodiesel reaction scheme

The transesterification reaction is affected by the molar ratio of glycerides to alcohol, the catalyst, reaction temperature, reaction time, and the free fatty acids content and water content of the oils or fats.

Biodiesels produced from lipid sources are mainly comprised of six different FAE's, consisting of palmitic acid (C16:0), steric acid (C18:0), oleic acid (C18:1), linoleic acid (C18:2) and linoleic acid (C18:3) alkyl esters, with small amounts of palmitoleic acid (C16:1) also present. Ideal biodiesel fuels mainly contain high amounts of methyl oleate, methyl palmitoleate, and ethyl palmitate [1], [9]. In this study, the phase equilibria for mixtures of CO_2 + ethyl palmitate was investigated. Besides the potential for non-catalytic biodiesel production at high pressures (in the supercritical state), supercritical CO_2 also offers an exciting alternative to purification and glycerol separation in water-free processes [10], [11].

Ethyl palmitate fatty acid ethyl esters are produced in the palmitic acid transesterification process in the presence of ethanol.

Fig. 2 shows the molecular structure of ethyl palmitate.
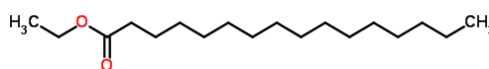

Fig. 2 Molecular structure of ethyl pamitate FAEE

M. A. Sedghamiz and S. Raeissi are with School of Chemical and Petroleum Engineering, Shiraz University, Shiraz, Iran (e-mail: sedghamiz.ma@gmail.com, raeissi@shirazu.ac.ir).

World Academy of Science, Engineering and Technology
International Journal of Chemical and Molecular Engineering
Vol:8, No:2, 2014

II. THERMODYNAMIC MODELING

The modeling of experimental equilibrium data was investigated using the PR (PR) equation of state, combined with two different mixing rules, consisting of the Van der Waals conventional mixing rule (vdW1) and the Wong-Sandler (WS) mixing rule. In order to predict the phase equilibrium for non-ideal systems, the WS mixing rule requires the use of a Gibb's excess energy (G^E) model, in order to combine a liquid activity model with an equation of state. Mixtures of CO_2 and FAEE have non-ideal behavior due to the presence of a long-chained FAEE, together with the small CO_2 molecule. As a result, the WS-G^E mixing rule should be able to predict the phase behavior of this system accurately.

The classical vdW1f mixing rules, as well as activity coefficient models like the Margules and van Laar equations, use 'average' or 'overall' compositions. They are models based on 'random mixing' [12]-[14]. However, due to intermolecular forces, the mixing of molecules is never entirely random and a way to account for the non-randomness can lead to improved models and better descriptions of phase behavior [10], [12], [15], [16]. Therefore, local composition activity coefficient models have drastically changed the range of applicability of liquid phase models.

Some of the most common G^E models include the NRTL and UNIQUAC models. The NRTL model is based on the critical properties of the components and the UNIQUAC model is based on area and volume parameters. FAEEs have known critical properties (T_c, P_c) and ω, but determining their surface and volume parameters is more challenging. Because of this, different methods have been investigated for the determination of these two unknown variables. In this study, a group contribution method has been used to calculate the surface and volume parameters (r, q) for ethyl palmitate FAEE.

The thermodynamic models used, including the Peng-Robinson equation of state, and the mixing rules are presented below [12]:

A. PR Equation of State:

The Peng-Robinson EOS is used to predict the phase equilibria of the binary system of CO_2 + ethyl palmitate. Equations (1) and (2) represent the Peng-Robinson EOS and its parameters.

$$P = \frac{RT}{v-b} - \frac{a(T)}{v(v+b)+b(v-b)} \tag{1}$$

where:

$$
\begin{aligned}
a(T) &= a_c \alpha \\
a_c &= 0.45724 \frac{(RT_c)^2}{P_c} \\
\alpha &= [1+m(1-\sqrt{T_r})]^2 \\
b &= 0.07780 \frac{RT_c}{P_c} \\
m &= 0.37464 + 1.54226\omega - 0.26992\omega^2
\end{aligned}
\tag{2}
$$

B. Van der Waals Mixing Rule

Equations (3) and (4) give the mixing rules and combining laws used in the vdW1 model.

$$
\begin{aligned}
a &= \sum_{i=1}^{n} \sum_{j=1}^{n} x_i x_j a_{ij} \\
b &= \sum_{i=1}^{n} \sum_{j=1}^{n} x_i x_j b_{ij}
\end{aligned}
\tag{3}
$$

where:

$$
\begin{aligned}
a_{ij} &= \sqrt{a_i a_j}\,(1-k_{ij}) \\
b_{ij} &= \frac{b_i + b_j}{2}(1-l_{ij})
\end{aligned}
\tag{4}
$$

in which l_{ij} and k_{ij} are binary interaction parameters that are optimized to the experimental phase equilibrium data for the CO_2+FAEE system.

C. Wong Sandler Mixing Rule

The Wong-Sandler mixing rule, developed for cubic equations of state, equates the excess Helmholtz free energy at infinite pressure from an equation of state to that from an activity coefficient model [12], [17].

$$
\begin{aligned}
a &= b\left(\sum_i x_i \frac{a_i}{b_i} + \frac{A^E}{0.623}\right) \\
b &= \frac{\sum_i \sum_j x_i x_j (b - \frac{a}{RT})_{ij}}{1 + \frac{A^E}{RT} - \sum_i x_i \frac{a_i}{b_i RT}}
\end{aligned}
\tag{5}
$$

where:

$$
\left(b - \frac{a}{RT}\right)_{ij} = \frac{(b_i - \frac{a_i}{RT}) + (b_j - \frac{a_j}{RT})}{2}(1-k_{ij}) \tag{6}
$$

$G^E = A^E$ and k_{ij} is an optimizing parameter.

D. Activity Models

The excess energy was calculated in this study by two different activity models, namely NRTL and UNIQUAC. Equations (7)-(11) represents these two activity models and the relations to calculate their parameters [12].

E. NRTL Activity Model

$$\frac{g^E}{RT} = x_1 x_2 \left(\frac{\tau_{12} G_{12}}{x_1 + x_2 G_{21}} + \frac{\tau_{12} G_{12}}{x_2 + x_1 G_{12}}\right) \tag{7}$$

where:

$$
\begin{aligned}
\tau_{12} &= \frac{\Delta g_{12}}{RT} \quad \tau_{21} = \frac{\Delta g_{21}}{RT} \\
\ln G_{12} &= -\alpha_{12}\tau_{12} \quad \ln G_{21} = -\alpha_{12}\tau_{21} \\
\tau_{11} &= \tau_{22} = 0, \quad G_{11} = G_{22} = 0, \quad \alpha_{12} = \alpha_{21}
\end{aligned}
\tag{8}
$$

and $\Delta g_{12}, \Delta g_{21}, \alpha_{12}$ are the binary parameters.

World Academy of Science, Engineering and Technology
International Journal of Chemical and Molecular Engineering
Vol:8, No:2, 2014

F. UNIQUAC Activity Mode

$$g^E = g^E(combinatorial) + g^E(residual)$$

$$\frac{g^E(combinatorial)}{RT} = x_1 \ln \frac{\Phi_1}{x_1} + x_2 \ln \frac{\Phi_2}{x_2} + \frac{z}{2}(q_1 x_1 \ln \frac{\theta_1}{\Phi_1} + q_2 x_2 \ln \frac{\theta_2}{\Phi_2}) \quad (9)$$

$$\frac{g^E(residual)}{RT} = -q_1 x_1 \ln[\theta_1 + \theta_2 \tau_{21}] - q_2 x_2 \ln[\theta_2 + \theta_1 \tau_{12}]$$

where:

$$\Phi_1 = \frac{x_1 r_1}{x_1 r_1 + x_2 r_2}$$

$$\theta_1 = \frac{x_1 q_1}{x_1 q_1 + x_2 q_2} \quad (10)$$

$$\ln \tau_{21} = -\frac{\Delta u_{21}}{RT}, \quad \ln \tau_{12} = -\frac{\Delta u_{12}}{RT}$$

r and q are pure component parameters, the coordination number, z, is taken to be 10, and $\Delta u_{12}, \Delta u_{21}$ are binary parameters to be optimized.

The Hansen group contribution method for the estimation of r and q is [18]:

$$r_i = \sum_k v_k^{(i)} R_k, \quad q_i = \sum_k v_k^{(i)} Q_k \quad (11)$$

where $v_k^{(i)}$ is the number of groups of type k in molecule i and R_k and Q_k are dimensionless surface and volume group parameters.

G. Optimizing Parameters

Each approach has parameters which are optimized to experimental data with an objective function as defined by equation (12) that calculates the minimum deviation between predicted values from the corresponding experimental data.

$$OF_{Temp.} = \frac{\left| P_{bubble}^{exp.} - P_{bubble}^{cal.} \right|}{P_{bubble}^{exp.}} \times 100 \quad (12)$$

The thermodynamic models were programmed in MATLAB and the optimizing procedure was done using the Differential Evaluation (DE) algorithm.

The experimental bubble pressure data for a binary system of CO_2+ethyl palmitate at high pressures were taken from literature [11] in order to evaluate the models and optimize the interaction parameters. CO_2 mole fractions were in the range of 0.5033 to 0.9913. Temperatures ranged from 313.15 to 353.15 K and pressure went up to 21 MPa [11].

Table I presents the properties of CO_2 and FAEE which were used in the modeling [11].

III. Results

The UNIQUAC volume and surface parameters, predicted by the group contribution method are given in Table II [18].

Each approach involved optimizing its own set of binary parameters. Table III shows the optimized parameters at each temperature.

TABLE I
THERMODYNAMIC PROPERTIES OF CO_2 AND FAEE

Specification	Molecule	
	CO_2	Ethyl Palmitate
T_c (K)	304.21	765.177
P_c (MPa)	7.38	1.31288
ω	0.2236	0.9019
r	3.26	12.9202
q	2.38	10.676
Mw (g/mol)	44.01	248.48

TABLE II
GROUP CONTRIBUTION PARAMETERS FOR ETHYL PALMITATE FAEE

Group numbers					
Main	Secondary	Name	Volume R_k	Surface area Q_k	$v_k^{(i)}$
1	1	CH_3	0.9011	0.848	2
	2	CH_2	0.6744	0.540	14
11	22	CH_2COO	1.6764	1.420	1

TABLE III
OPTIMIZED BINARY PARAMETERS AT EACH TEMPERATURE

Method	Temperature (K)	Optimized binary parameters			
		k_{ij}	α_{ij}	Δg_{12}	Δg_{21}
NRTL	313.15	0.0532	0.34572	39.456	2784.345
	323.15	0.0635	0.36896	-14.386	2541.647
	333.15	0.0689	0.39264	-83.574	2256.932
	343.15	0.0835	0.43275	-67.635	2087.163
	353.15	0.0946	0.46367	-142.567	1965.703
		k_{12}	Δu_{12}	Δu_{21}	
UNIQUAC	313.15	0.1115	1882.197	-439.201	
	323.15	0.1109	1847.934	-475.724	
	333.15	0.1185	1891.222	-531.722	
	343.15	0.1321	1486.754	-314.053	
	353.15	0.1488	1072.661	-31.5021	
		k_{ij}			
PR-vdw1	313.15	0.0482			
	323.15	0.0464			
	333.15	0.0492			
	343.15	0.0605			
	353.15	0.0719			

The bubble pressure results of the three thermodynamic models were compared to experimental values from the literature. Figs. 3-7 show a comparison between the different approaches at various temperatures.

To compare the results, average absolute deviations, and average relative deviations were also calculated at different temperatures for each approach and the results are presented in Table IV.
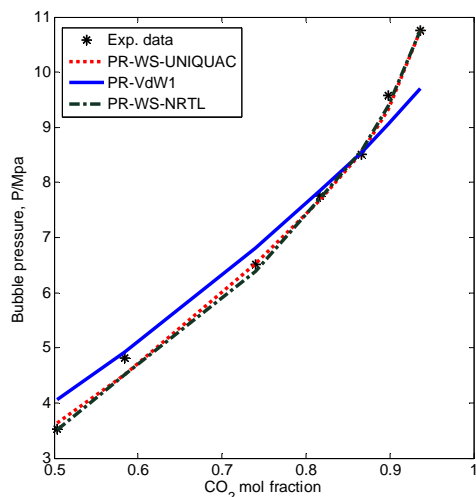
World Academy of Science, Engineering and Technology
International Journal of Chemical and Molecular Engineering
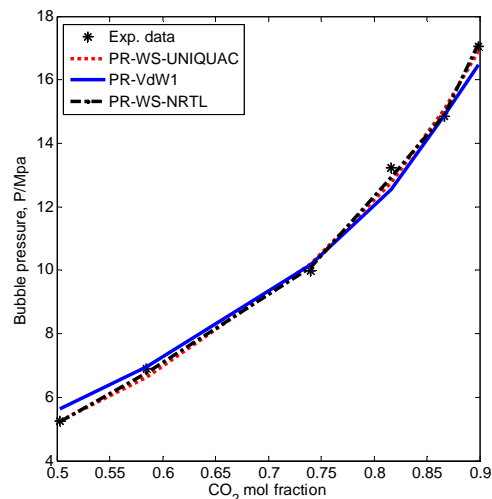Vol:8, No:2, 2014

Fig. 3 Bubble pressure for the system of CO_2+FAEE vs. mole fraction of CO_2 at a temperature of 313.15 K
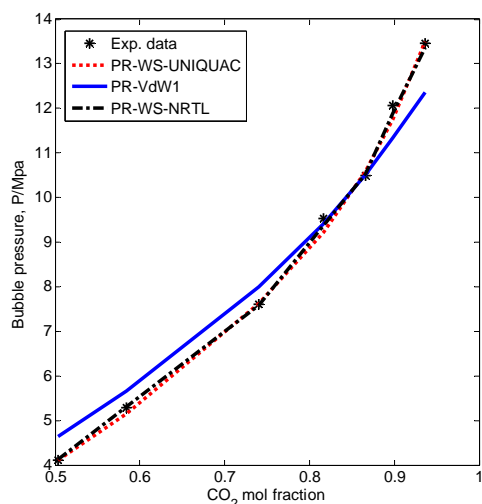

Fig. 4 Bubble pressure for the system of CO_2+FAEE vs. mole fraction of CO_2 at a temperature of 323.15 K

Fig. 5 Bubble pressure for the system of CO_2+FAEE vs. mole fraction of CO_2 at a temperature of 333.15 K
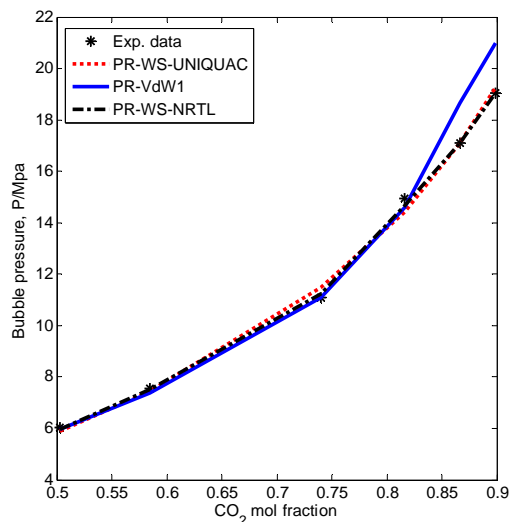

Fig. 6 Bubble pressure for the system of CO_2+FAEE vs. mole fraction of CO_2 at a temperature of 343.15 K
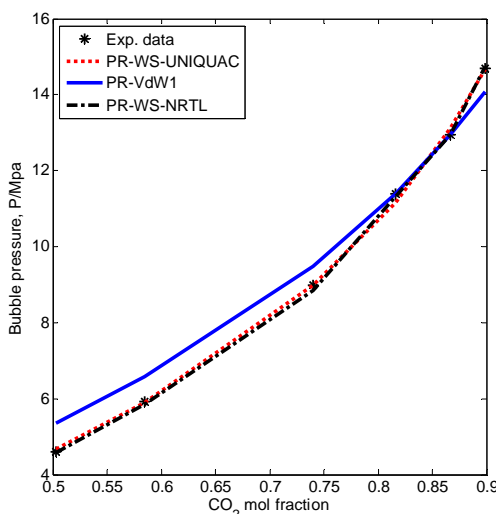

Fig. 7 Bubble pressure for the system of CO_2+FAEE vs. mole fraction of CO_2 at a temperature of 353.15 K

TABLE IV
AVERAGE ABSOLUTE AND RELATIVE DEVIATIONS AT DIFFERENT TEMPERATURES FOR THE THREE MODELS

Method	Temperature (K)	AAD	ARD%
	313.15	0.12	1.71
	323.15	0.08	0.79
NRTL	333.15	0.05	0.65
	343.15	0.11	1.09
	353.15	0.09	0.87
	313.15	0.11	1.94
	323.15	0.13	1.47
UNIQUAC	333.15	0.09	0.95
	343.15	0.22	1.98
	353.15	0.23	1.97
	313.15	0.38	5.54
	323.15	0.36	5.46
PR	333.15	0.42	6.22
	343.15	0.32	4.16
	353.15	0.43	3.96

World Academy of Science, Engineering and Technology
International Journal of Chemical and Molecular Engineering
Vol:8, No:2, 2014

IV. CONCLUSIONS

The PR EOS with classical mixing rules shows the maximum deviations from experimental data, which can be related to the limitation of this EOS in modeling long-chained molecules such as FAEEs. This dramatic deviation can be seen at all temperatures.

The two approaches using the Wong-Sandler mixing rule showed that this approach has less errors than the conventional Van der Waals mixing rule. According to results, the NRTL G^E model led to the least errors due to the accurate thermodynamic properties, while the UNIQUAC model showed higher errors, perhaps because of the non-accurate binary interaction parameters.

NOMENCLATURE

a	energy term
A	Helmholtz energy
b	co-volume parameter
G	Gibbs free energy
g	molar Gibbs energy
k_{ij}	binary interaction parameter
l_{ij}	binary interaction parameter
P	pressure
q	surface parameter
R	universal gas constant
r	volume parameter
T	temperature
v	molar volume
x_i	molar composition of component i
z	coordination number
Greek letters	
α_{12}	reduced energy
Θ_1	surface area fraction for component 1 in the mixture
τ_{12}	Boltzmann factor
ω	acentric factor
Φ_1	volume fraction for component 1 in the mixture
Superscripts and subscripts	
i,j	component
1,2	denotes CO_2 and FAEE
c	critical properties
r	reduced property
E	excess property
Cal.	calculated parameters
Exp.	experimental data

REFERENCES

[1] Sharma, Y.C., B. Singh, and S.N. Upadhyay, *Advancements in development and characterization of biodiesel: A review.* Fuel, 2008. 87(12): p. 2355-2373.
[2] Halim, R., M.K. Danquah, and P.A. Webley, *Extraction of oil from microalgae for biodiesel production: A review.* Biotechnol Adv, 2012. 30(3): p. 709-32.
[3] Williams, P.J.l.B. and L.M.L. Laurens, *Microalgae as biodiesel & biomass feedstocks: Review & analysis of the biochemistry, energetics & economics.* Energy & Environmental Science, 2010. 3(5): p. 554.
[4] Saxena, P., S. Jawale, and M.H. Joshipura, *A Review on Prediction of Properties of Biodiesel and Blends of Biodiesel.* Procedia Engineering, 2013. 51: p. 395-402.
[5] Talebian-Kiakalaieh, A., N.A.S. Amin, and H. Mazaheri, *A review on novel processes of biodiesel production from waste cooking oil.* Applied Energy, 2013. 104: p. 683-710.
[6] Rustan, A.C. and C.A. Drevon, *Fatty Acids: Structures and Properties.* 2005.
[7] Anitescu, G. and T.J. Bruno, *Fluid properties needed in supercritical transesterification of triglyceride feedstocks to biodiesel fuels for efficient and clean combustion – A review.* The Journal of Supercritical Fluids, 2012. 63: p. 133-149.
[8] Hoekman, S.K., et al., *Review of biodiesel composition, properties, and specifications.* Renewable and Sustainable Energy Reviews, 2012. 16(1): p. 143-169.
[9] Nasir, N.F., et al., *Process system engineering in biodiesel production: A review.* Renewable and Sustainable Energy Reviews, 2013. 22: p. 631-639.
[10] Pinto, L.F., et al., *Phase equilibrium data and thermodynamic modeling of the system (CO2+biodiesel+methanol) at high pressures.* The Journal of Chemical Thermodynamics, 2012. 44(1): p. 57-65.
[11] Gaschi, P.S., et al., *Phase equilibrium measurements and thermodynamic modelling for the system (CO2+ethyl palmitate+ethanol) at high pressures.* The Journal of Chemical Thermodynamics, 2013. 57: p. 14-21.
[12] Kontogeorgis, G. and G. Folas, *Thermodynamic Models for Industrial Applications From Classical and Advanced Mixing Rules to Association Theories* 2010.
[13] Santiago, R.S., G.R. Santos, and M. Aznar, *UNIQUAC correlation of liquid–liquid equilibrium in systems involving ionic liquids: The DFT–PCM approach.* Fluid Phase Equilibria, 2009. 278(1-2): p. 54-61.
[14] Follegatti-Romero, L.A., et al., *Liquid–liquid equilibria for ethyl esters+ethanol+water systems: Experimental measurements and CPA EoS modeling.* Fuel, 2012. 96: p. 327-334.
[15] Oliveira, M.B., et al., *Modeling Phase Equilibria Relevant to Biodiesel Production: A Comparison ofgEModels, Cubic EoS, EoS−gEand Association EoS.* Industrial & Engineering Chemistry Research, 2011. 50(4): p. 2348-2358.
[16] Basso, R.C., et al., *LLE experimental data, thermodynamic modeling and sensitivity analysis in the ethyl biodiesel from macauba pulp oil settling step.* Bioresour Technol, 2013. 131: p. 468-75.
[17] Coutsikos, P., N.S. Kalospiros, and D.P. Tassios, *Capabilities and limitations of the Wong-Sandler mixing rules.* Fluid Phase Equilibria, 1995. 108(1–2): p. 59-78.
[18] Bruce E. Poling, John M. Prausnitz, and J.P. OConnell, *The Properties of Gases and Liquids, Fifth Edition.* 2001.